Partially Unfolded Species Populated during Equilibrium Denaturation of the β-Sheet Protein Y74W Apo-Pseudoazurin†

Susan Jones,[‡,§] John S. Reader,[‡,§,||] Maria Healy,[⊥] Andrew P. Capaldi,[§] Alison E. Ashcroft,[§] Arnout P. Kalverda,[§] D. Alastair Smith,[⊥] and Sheena E. Radford*[,§]

School of Biochemistry and Molecular Biology, and Department of Physics and Astronomy, University of Leeds, Leeds LS2 9JT, England

Received October 14, 1999; Revised Manuscript Received February 8, 2000

ABSTRACT: Apo-pseudoazurin is a single domain cupredoxin. We have engineered a mutant in which a unique tryptophan replaces the tyrosine residue found in the tyrosine corner of this Greek key protein, a region that has been proposed to have an important role in folding. Equilibrium denaturation of Y74W apo-pseudoazurin demonstrated multistate unfolding in urea (pH 7.0, 0.5 M Na_2SO_4 at 15 °C), in which one or more partially folded species are populated in 4.3 M urea. Using a variety of biophysical techniques, we show that these species, on average, have lost a substantial portion of the native secondary structure, lack fixed tertiary packing involving tryptophan and tyrosine residues, are less compact than the native state as determined by fluorescence lifetimes and time-resolved anisotropy, but retain significant residual structure involving the trytophan residue. Peptides ranging in length from 11 to 30 residues encompassing this region, however, did not contain detectable nonrandom structure, suggesting that long-range interactions are important for stabilizing the equilibrium partially unfolded species in the intact protein. On the basis of these results, we suggest that the equilibrium denaturation of Y74W apo-pseudoazurin generates one or more partially unfolded species that are globally collapsed and retain elements of the native structure involving the newly introduced tryptophan residue. We speculate on the role of such intermediates in the generation of the complex Greek key fold.

The mechanism of protein folding has been the subject of much debate and intensive study in recent years. Studies of the refolding of proteins in vitro following their dilution from chemical denaturants, combined with protein engineering and solvent perturbation methods, have begun to provide insights into the nature of the complex events that accompany the transition between the denatured and native states of a protein. Although for most small proteins folding is a highly cooperative event, proteins over 100 residues in length (*1*), and some smaller proteins (*2*−*5*), populate intermediates in the first msec of folding. These species usually contain substantial secondary structure but lack the fixed tertiary interactions that characterize the native state, although their rapid formation makes higher resolution information difficult to obtain. For a number of proteins, intermediates have been detected under equilibrium conditions (*5*−*12*), offering opportunities to determine more detailed information about the conformational properties of partially folded states and the roles of domains and subdomains in folding, especially for those proteins for which kinetic and equilibrium species have been shown to be similar (*6*, *13*, *14*).

Until recently, the majority of folding studies focused on α-helical or mixed α/β-proteins. By contrast with these, some β-sheet proteins, particularly those with complex topologies, are stabilized by longer range interactions, posing intriguing questions about how these interactions form during folding (*15*, *16*). Studies on a number of β-sheet proteins have now shown that, like their helical and mixed α/β-counterparts, small β-sheet proteins usually fold in the absence of intermediates (*17*−*23*) while larger, more complex β-sheet proteins populate intermediates during refolding (*24*−*33*). Several models have been proposed to explain how β-strands distant in sequence space might form during folding, in particular for the common Greek key fold. These include the initial formation of a long β-hairpin that later twists into the classic Greek key motif (*34*) and models involving initiation by the formation of a "β-zipper" involving hydrophobic stacking between non-hydrogen-bonded β-strands on opposite sides of the β-barrel (*35*). Whether either, or both, of these models are relevant for Greek key folding has not yet been discerned, but recent investigations have demonstrated β-hairpin formation and β-turn formation (between unpaired β-strands) in peptides in isolation (*36*−*38*). Additionally, a common but unique feature of most Greek key proteins is the "tyrosine corner" (*39*). Here, a tyrosine residue (Y) at the beginning or end of an antiparallel β-strand makes a hydrogen bond from its side-chain hydroxyl group to the

† S.J. and J.S.R. were supported by the BBSRC, and M.H. by the University of Leeds. A.P.K. and A.E.A. are funded by the Wellcome Trust. D.A.S. and S.E.R. acknowledge financial support from the BBSRC, EPSRC, and the Wellcome Trust. The work is a contribution from the Astbury Centre for Structural Molecular Biology and the North of England Structural Biology Centre, which is funded by the BBSRC.

* To whom correspondence should be addressed. Phone (+44) 113 233 3170. Fax (+44) 113 233 3167. E-mail s.e.radford@leeds.ac.uk.

‡ These authors contributed equally to the work.

§ School of Biochemistry and Molecular Biology, University of Leeds, Leeds LS2 9JT, U.K.

|| Current address: The Scripps Research Institute, 10550 North Torrey Pines Road, La Jolla, CA 92037.

⊥ Department of Physics and Astronomy, University of Leeds, Leeds LS2 9JT, U.K.

10.1021/bi9923959 CCC: $19.00
Published on Web 04/21/2000

backbone amide and/or carbonyl of a residue at position Y-3, Y-4, or Y-5. This motif is found in over 40 different Greek key proteins from both eukaryotes and prokaryotes. In addition, four Greek key proteins have been reported to have "tryptophan corners" (*39*), where tryptophan replaces the tyrosine residue. As a consequence of its high conservation, the tyrosine corner has been postulated to be important in folding and/or stabilization of the native protein (*39*). This hypothesis has been supported by recent experiments on the folding of fibronectin type III domains and the related Ig-superfamily, both of which retain a conserved tyrosine corner (*40*). These studies have shown that for both these proteins the tyrosine corner is important for stabilizing the native structure, but only in the former case is it important for folding.

In this paper, we investigate the folding of pseudoazurin from *Paracoccus pantotrophus* (in the absence of its copper ion, named apo-pseudoazurin). The protein contains eight β-strands arranged in a complex double-wound Greek key fold and two α-helices (Figure 1a). In accordance with the Hazes and Hol model (*35*), strands VI and VII of apo-pseudoazurin form a putative β-zipper that also contains the tyrosine corner in which Tyr74 is hydrogen bonded to the backbone carbonyl of Glu70 (Figure 1b). The tyrosine corner is found in all blue-copper proteins at an equivalent location involving a Greek key connection that is opposite the copper-binding site. To investigate the role of this region in the folding and stability of apo-pseudoazurin, Tyr74 was replaced with a tryptophan residue, providing a unique fluorescent probe to follow protein folding (the wild-type protein lacks tryptophan residues). We show that the mutation does not disrupt the native structure of apo-pseudoazurin. Introduction of the tryptophan, however, alters the equilibrium unfolding behavior of the protein such that intermediate(s) becomes populated during denaturation. Further analysis reveals these species to be partially structured as determined by fluorescence and circular dichroism and to retain residual structure involving the newly introduced tryptophan residue, as revealed by fluorescence anisotropy measurements. On the basis of these results, we speculate on the possible role of protein collapse and burial of hydrophobic residues during the early stages of folding of apo-pseudoazurin and the importance of the tyrosine corner and its associated regions in acquisition of this Greek key fold.

MATERIALS AND METHODS

Chemicals. All chemicals were purchased from Sigma Chemical Co., except for urea (ultrapure grade), which was obtained from ICN Pharmaceuticals. T4 DNA polymerase and T4 DNA ligase were purchased from Promega. DNA was prepared using Wizard mini-plasmid DNA kit (Promega) and manually sequenced using Sequenase version 2.0 from Amersham.

Mutation of Pseudoazurin. Y74 was mutated to tryptophan using the Kunkel method of mutagenesis (*41*). Briefly, the uracil-containing single-stranded DNA of plasmid pJR2 (*42*) was prepared from *Escherichia coli* strain RZ1032 and the MUT1 oligonucleotide (5′ CGGGGCTTTGGGGCGTGAA-ATG 3′) annealed (at position 634−655), extended, and ligated. The mutated plasmid (pMut1) was then transformed into *E. coli* XL1-blue and successful mutagenesis confirmed by DNA sequencing of the resulting plasmid DNA.

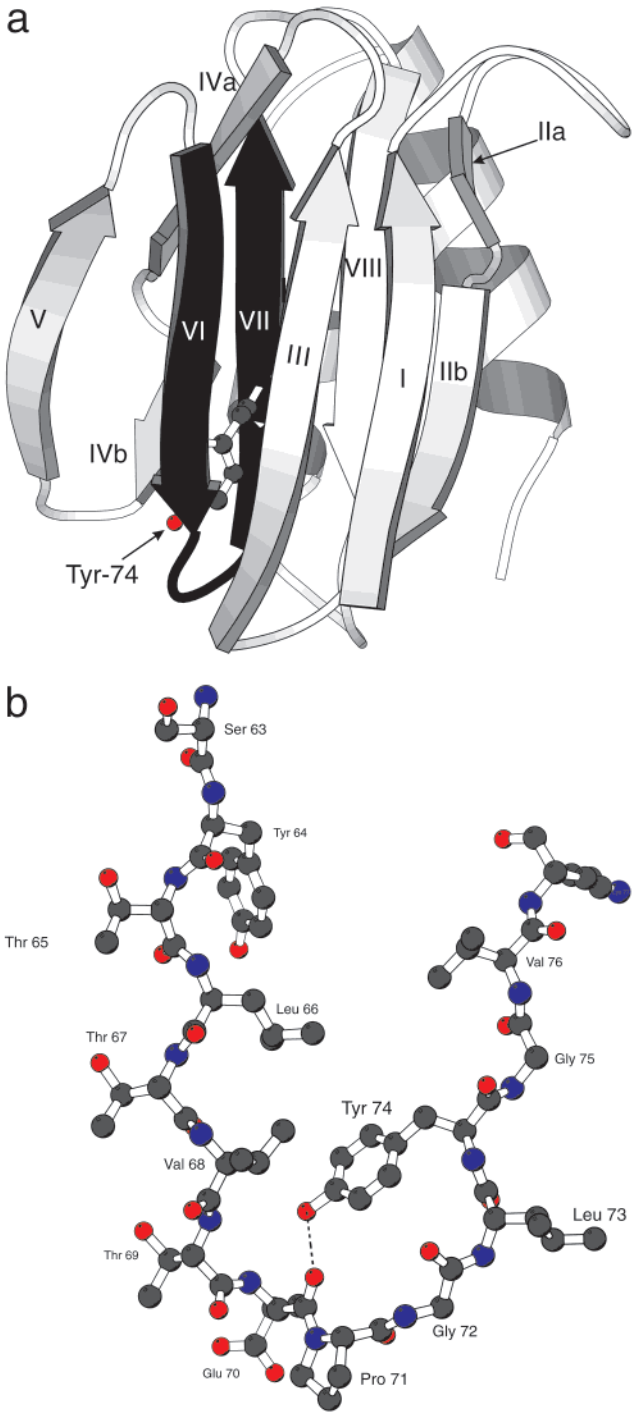

FIGURE 1: Structure of (a) wild-type apo-pseudoazurin, produced from the crystal structure using the program MOLSCRIPT (*81*) (Brookhaven protein databank accession code 1ADW). Strands VI and VII of the structure are shown in black. (b) Segment of pseudoazurin encompassing residues 63−77 of strands VI and VII. The hydrogen bond between the hydroxyl group of Tyr74 and the backbone carbonyl group of Glu70 (the tyrosine corner) is shown.

Preparation of Y74W Apo-Pseudoazurin. The Y74W[1] pseudoazurin was overexpressed from plasmid pMut1 in *E. coli* strain XL1-blue. The cells were grown in 2xTY media, supplemented with 1mM $CuSO_4$ at 37 °C for 24 h without

[1] Abbreviations: ESI MS, electrospray ionisation mass spectrometry; ICP MS, inductively coupled plasma mass spectrometry; ANS, 1-anilino-8-naphthalenesulphonic acid; Y74W apo-pseudoazurin, apo-pseudoazurin containing the mutation of Tyr74 to tryptophan.

induction. The protein was purified and the copper removed as described in ref *27*. SDS−PAGE and electrospray ionization mass spectrometry (ESI MS) (using a Micromass Platform II mass spectrometer) showed the protein to be greater than 98% pure and no residual copper remained bound to the protein. Further analysis of metal ion content by inductively coupled plasma mass spectrometry (ICP-MS) showed that ~0.3% copper and ~0.8% zinc remained bound to the protein. Sedimentation velocity ultracentrifugation also showed the protein in buffer A at 15 °C (see below) to be monodisperse and of the expected molecular weight.

Equilibrium Denaturation of Y74W Apo-Pseudoazurin. Far-UV CD and fluorescence measurements were performed using 0.6 or 0.1 mg/mL protein, respectively, in buffer A (20m M sodium phosphate, 0.5 M Na_2SO_4 and 1 mM DTT, pH 7.0) containing the appropriate concentrations of urea. All experiments were reproducibly carried out in triplicate on different protein preparations, and the data were averaged. All solutions were incubated at 15 °C for at least 12 h prior to their measurement. All steady-state CD experiments were performed on a Jasco J-715 spectropolarimeter with a Jasco PTC-348W peltier system for temperature control. The CD signal at 220 nm (1 nm band width) was measured for 3 min in a 1 mm path length cuvette and the data averaged. Fluorescence experiments were carried out on a Perkin-Elmer LS50B luminescence spectrometer using 1 cm path length cuvettes. Fluorescence was excited at 280 nm using slit widths of 3 nm. Fluorescence emission was measured for 3 min at 335 nm, and the resulting data were averaged.

The pre- and posttransition baselines measured for both far-UV CD and fluorescence equilibrium denaturation were linear and had very small slopes (see Supporting Information, Figure 1), indicating the absence of multiple native states with different global stabilities under the conditions used. To allow comparison of the unfolding transitions monitored by the different spectroscopic techniques the data were converted to the percentage native signal versus urea concentration using eq 1:

$$\%\text{native signal} = \frac{\text{Obs(xMurea)} - \text{D(xMurea)}}{\text{N(xMurea)} - \text{D(xMurea)}} \times 100\% \quad (1)$$

where, D(xMurea) is the signal of the denatured state; N(xMurea) is the signal of the native state, and Obs(xM urea) is the observed signal at each urea concentration. Values of $\Delta G_{un}^{H_2O}$ and m_{un} were determined using eq 2

$$(\text{signal}) = [(a[\text{den}] + b)e^{(\Delta G_{un}^{H_2O} - m_{un}[\text{den}])/RT)} + (c[\text{den}] + d)]/(1 + e^{(\Delta G_{un}^{H_2O} - m_{un}[\text{den}])/RT}) \quad (2)$$

[where $\Delta G_{un}^{H_2O}$ is the free energy in water (containing 0.5M Na_2SO_4) between the unfolded and native states; m_{un} is the denaturant dependence of the free energy, that is proportional to the surface-area exposed upon unfolding; *b* and *d* are the signals of the unfolded and folded states respectively in the absence of denaturant; and *a* and *c* are the change of these signals with denaturant concentration [*den*]] (*43*).

Dynamic Light Scattering. Dynamic light-scattering experiments were carried out using a Polymer Laboratories BD-2000 dynamic light-scattering apparatus. Protein solutions of 10, 5, and 1 mg/mL in buffer A containing 4.3 M urea were analyzed after filtration using a 0.2 μm filter to remove dust particles. A sample time of 8.0 s, last channel of 1024, and mass-normalization set to 3.00 (for globular species) were used. Fifty accumulations for each solution were acquired to produce an average hydrodynamic radius (nm) calculated according to the manufacturers specifications.

NMR Spectroscopy. ^{1}H NMR spectra were recorded at 15 °C on a Varian Inova 500 MHz NMR spectrometer. Samples contained 0.5 mM Y74W apo-pseudoazurin in buffer A containing 0, 4.3, or 8 M urea. Each sample was equilibrated at 15 °C overnight. Proton NMR spectra were acquired with 512 transients using presaturation during the 1.5 s recycle delay to suppress the water signal. The spectral width was 6982.6 Hz and 256 scans were taken with an acquisition time of 1.17 s. The data were processed using the package Felix 2.3 (Biosym Technologies, San Diego).

Fluorescence Lifetime and Time-Resolved Anisotropy. Fluorescence lifetimes and time-resolved anisotropy decays of 0.1 mg/mL (7.4 μM) Y74W apo-pseudoazurin in buffer A containing 0 M to 8 M urea were measured at 15 °C. Measurements were made using the time-correlated single photon-counting technique with an Edinburgh Instruments FL900DCT fluorescence spectrometer incorporating a Hamamatsu R3809 microchannel plate photomultiplier tube. The excitation source was a cavity-dumped dye laser, synchronously pumped by a frequency doubled mode locked Nd:YAG. The cavity dumped output from the dye laser was frequency doubled to produce an excitation source at 282 nm with a pulse width of approximately 8 picoseconds. The instrument response function had a full width half-maximum of ~ 50 ps.

The fluorescence decays, $I(t)$, (Table 1) were measured with the emission polarizer at the magic angle and were fitted by iterative reconvolution of the instrument function with a sum of exponentials of the form,

$$I(t) = \sum_{i=1}^{n} \beta_i \exp(-t/\tau_i) \quad (3)$$

where β_i are the amplitudes of the exponential function decay constants τ_i. The number of exponentials used, *n*, was the minimum required to achieve a good fit, which was assessed by examination of the sum of the residuals and the autocorrelation function in the conventional way.

Fluorescence anisotropy decays, $r(t)$, were calculated from the time-resolved decays with the emission intensity collected parallel, ($I_{||}$), and perpendicular, ($I_{\perp}$), to the vertically polarized excitation according to

$$r(t) = \frac{gI_{||}(t) - I_{\perp}(t)}{gI_{||}(t) + 2I_{\perp}(t)} \quad (4)$$

where the geometry factor of the spectrometer, *g*, was determined using horizontal excitation and was verified with a sample of aniline in methanol. To examine the fast and slow contributions to the fluorescence anisotropy decay, experiments were performed on two different time scales. A long time-scale experiment extending over 25 ns (Table

2) was used to determine rotational correlation times associated with global protein rotation, and a short time scale of 5 ns (Table 3) was used to investigate more accurately the contributions of faster segmental motion and tryptophan mobility. The anisotropy decays were fitted with either a single-exponential function or a sum of exponentials when a significant improvement in the fit justified their use. The well-known model incorporating the effect of local tryptophan motion and overall protein rotation in solution (*44*−*46*) on the decay of fluorescence anisotropy can strictly only be applied in certain cases where the absorption and emission dipole moments have known orientations with respect to the molecular axes. General models for anisotropy decay in complex systems that have more than one contribution from internal "wobbling" of the fluorophore and segmental motion are often intractable or the data obtained with current instrumentation cannot support the more complex analysis. In the simple case, when the time-resolved decay of fluorescence anisotropy, $r(t)$, can be fitted by a biexponential function of the form

$$r(t) = a_1 \exp(-t/\tau_1) + a_2 \exp(-t/\tau_2) \quad (5)$$

and $\tau_1 \ll \tau_2$, then τ_1 is usually associated with the rotational freedom of tryptophan in a cone of a semiangle, θ, given by

$$\frac{a_2}{a_1 + a_2} = \cos^2 \theta (1 + \cos \theta)^2/4 \quad (6)$$

and τ_2 is usually associated with the overall protein rotation in solution (*42*, *45*).

Y74W pseudoazurin peptides. Three peptides (RGT_{69}-EPGLWG_{75}GR) (pep1), (RGS_{63}YTLTVTEPGKWGVK_{77}GR) (pep2), and (RGG_{52}VESFKSKINESYTLTVTEPGKWGV-K_{77}GR) (pep3), 11, 19, and 30 residues in length, were synthesized. The peptides were designed to represent residues involved in the tyrosine corner of pseudoazurin with the following modifications: tryptophan replaced the tyrosine residue at position 74; a surface leucine residue (Leu73) was replaced by lysine to ensure an unequal positive and negative charge to improve solubility, and RG-end groups were added to provide repulsion of the end groups and avoid polymerization (*47*).

RESULTS

Purification and Characterization of Y74W Apo-Pseudoazurin. The Y74W mutation was introduced into the wild-type pseudoazurin gene (*pazS*) in the plasmid pJR2 (*48*), and the Y74W protein overexpressed and purified as described above. The yield of Y74W pseudoazurin was consistently lower than that of the wild-type protein (typically 10 mg of pure protein/L and 60 mg of pure protein/L, respectively). SDS−PAGE and ESI MS revealed a single protein species at the expected molecular mass for the holo-protein (13 428 ± 1 Da). To ensure that Y74W pseudoazurin had the same global tertiary structure as the wild-type protein, the absorbance spectra of the copper(II) species of the two proteins were compared. The spectra were identical (data not shown), apart from an increase in signal at 280 nm, consistent with incorporation of the indole group into the mutant protein. This indicates that the environment of the copper(II) ion in the two proteins is the same, and the precise arrangement of the copper ligands is retained in the mutant. In addition, the far-UV CD spectra (Figure 2), near-UV CD, and ^{1}H NMR spectra (data not shown) of the mutant protein both in the holo- and apo-forms are very similar to those of the wild-type protein, consistent with the retention of a highly native fold in both species, and indicating that removal of the copper ion does not perturb the native fold of the protein, consistent with fluorescence emission spectra (Figure 3) and previous X-ray results (*49*).

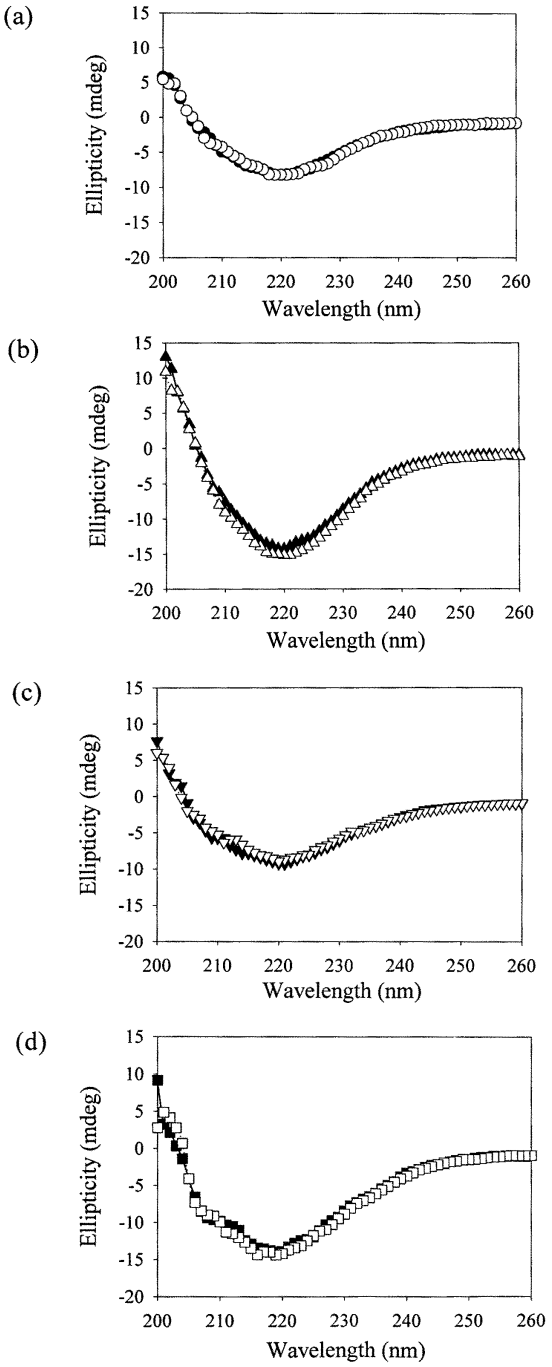

FIGURE 2: Far-UV circular dichroism spectra of wild-type and Y74W apo-pseudoazurin at pH 7.0 and 15 °C, with (open symbols) and without (closed symbols) 0.5 M Na_2SO_4. (a) Wild-type holo-pseudoazurin (CuII), (b) wild-type apo-pseudoazurin, (c) Y74W holo-pseudoazurin (CuII), and (d) Y74W apo-pseudoazurin.

Equilibrium Unfolding of Y74W Apo-Pseudoazurin. The equilibrium unfolding transitions of Y74W and wild-type apo-pseudoazurin, measured at pH 7.0, in the presence of

0.5 M Na_2SO_4, by far-UV CD at 220 nm are shown in Figure 4. The addition of Na_2SO_4 stabilizes the native states of wild-type and Y74W apo-pseudoazurin (Figure 2, Supporting Information). To ensure that the presence of stabilizing salt had no effect on the native conformations of either wild-type or Y74W pseudoazurin, far-UV CD and fluorescence emission spectra were analyzed in the presence and absence of 0.5 M Na_2SO_4. The data show that 0.5 M Na_2SO_4 does not perturb the native structures of either protein (Figures 2 and 3) in accord with ^{1}H NMR data (not shown). Note that, in the presence of the copper ion, both wild-type and Y74W apo-pseudoazurin proteins have a lower fluorescence signal than for the apo-proteins. This effect has been frequently observed for metallo-proteins (see ref *50*). All further experiments were thus carried out under these stabilizing conditions. For both wild-type and Y74W apo-pseudoazurin, unfolding is fully reversible under the chosen conditions. The equilibrium unfolding data for wild-type apo-pseudoazurin fit well to a simple, apparently two-state, transition (eq 2) with a $\Delta G_{un}^{H_2O}$ of 28.8 (±0.7) kJ/mol and an m_{un} value of 7.84 (±0.1) kJ/mol M, in agreement with previous results (*27*).

In comparison with the denaturation transition of the wild-type protein, Y74W apo-pseudoazurin unfolds in a more complex reaction, which cannot be described by a two-state transition (Figure 4). Rather, a plateau is observed between 4 and 5 M urea in the unfolding curve monitored by both far-UV CD and tryptophan fluorescence, suggesting that one or more intermediate species are populated during unfolding. In accord with this, equilibrium denaturation of Y74W apo-pseudoazurin at 25 °C in 0.5 M Na_2SO_4, although apparently fitting to a two-state transition, has a significantly decreased m_{un} value [4.99 (±0.59) kJ/mol M] compared with that of the wild-type protein [7.84 (±0.1) kJ/mol M] consistent with population of at least one intermediate species at equilibrium (data not shown) (*51*). Attempts to fit the data in Figure 4 to a simple three-state transition (N ⇌ I ⇌ U, where N, I, and U are native, intermediate, and unfolded species, respectively), although possible, were unsatisfactory since the stability of the protein and the sum of the *m*-values resulting from the fit were both substantially higher than expected (>50 kJ/mol and ∼14 kJ/mol M, respectively). The discrepancy in the fit can be explained by a number of scenarios. One possibility is that there are multiple native conformations. However, detailed analysis of the NMR spectra of the native protein showed only the expected number of resonances (not shown), analysis of the fluorescence anisotropy decay lifetimes of tryptophan show only a single decay component (see below), and the pretransition baseline of the denaturation curves is of shallow gradient and entirely linear (see Supporting Information, Figure 1), suggesting that such a scenario is unlikely. Alternatively, noncooperative denaturation of the intermediate species, contributions from cis/trans proline isomerization, or population of a number of intermediate species between 4 and 5 M urea would result in a simple three-state transition being inadequate to describe the unfolding data (*52*).

To ensure that the deviation from two-state unfolding behavior of Y74W apo-pseudoazurin was not attributable to intermolecular interactions or incomplete removal of copper ions during the preparation of the apo-protein, a series of

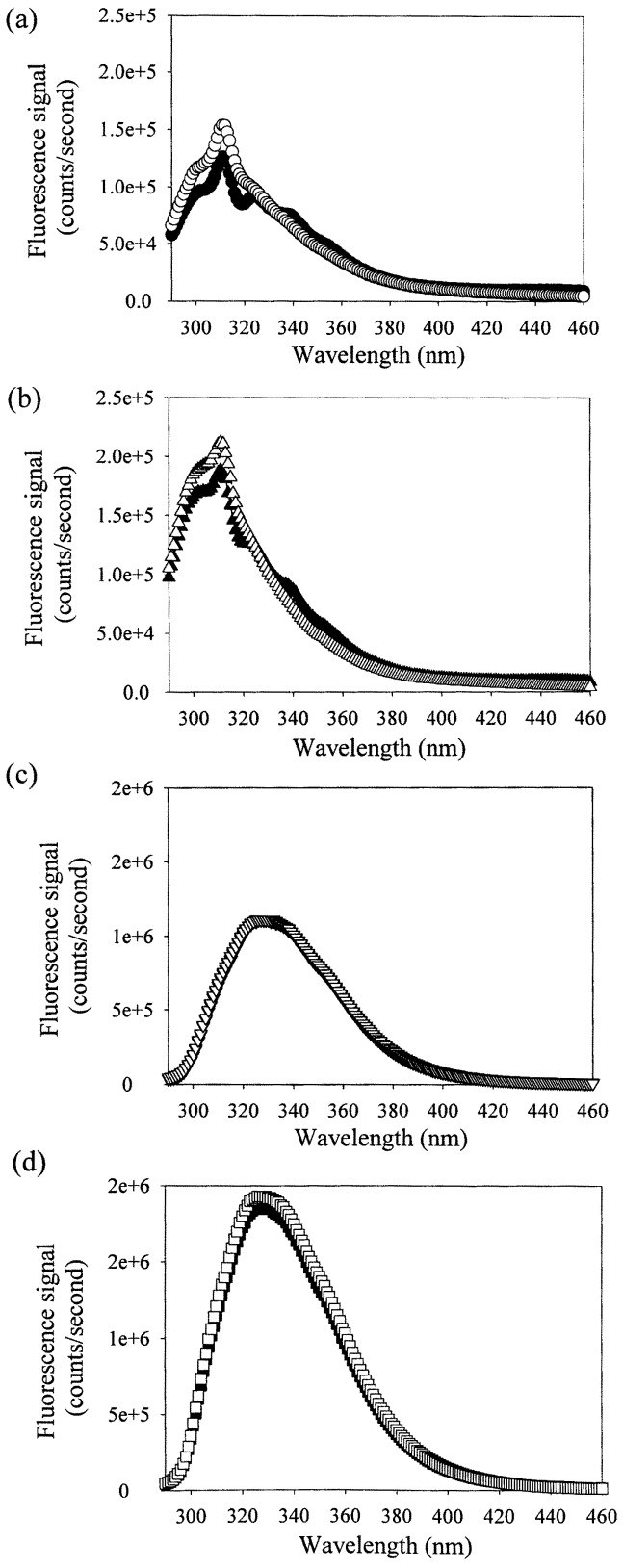

FIGURE 3: Fluorescence emission spectra of wild-type and Y74W apo-pseudoazurin at pH 7.0 and 15 °C, with (open symbols) and without (closed symbols) 0.5 M Na_2SO_4. (a) Wild-type holo-pseudoazurin (CuII). (b) Wild-type apo-pseudoazurin. (c) Y74W holo-pseudoazurin (CuII) and (d) Y74W apo-pseudoazurin. Fluorescence was excited at 280 nm. Note that wild-type pseudoazurin lacks tryptophan residues and the lower fluorescence signal allows visualization of the water Raman peak at 310 nm.

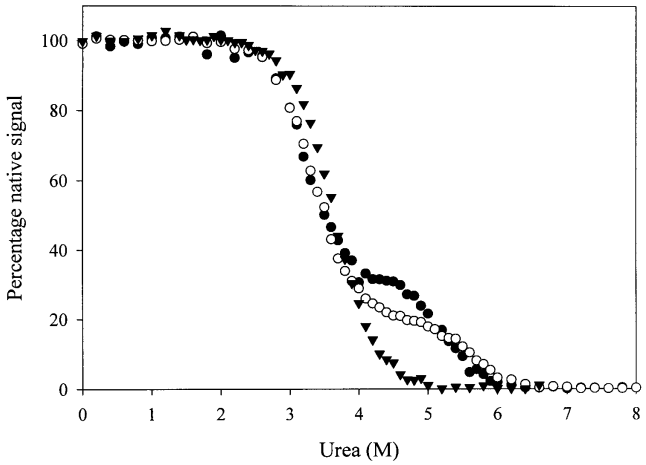

FIGURE 4: Urea-induced equilibrium unfolding of wild-type and Y74W apo-pseudoazurin at pH 7.0 and 15 °C, in 0.5 M Na_2SO_4. Far-UV circular dichroism of (▼) wild-type apo-pseudoazurin and (○) Y74W apo-pseudoazurin; tryptophan fluorescence (●) of Y74W apo-pseudoazurin. Na_2SO_4 was added to stabilize the proteins, all of which were fully unfolded in 2 M urea in the absence of Na_2SO_4 (see Figure 2, Supporting Information).

rigorous tests was carried out. Thus, the far-UV CD and tryptophan fluorescence signals of Y74W apo-pseudoazurin depend linearly upon protein concentration from 0.02 to 0.6 mg/mL in buffer A containing 0, 4.3, or 8 M urea. In addition, ANS does not bind to wild-type or Y74W apo-pseudoazurin in the presence of 4.3 M urea, ruling out minor populations of aggregated species (*53*). Dynamic light-scattering experiments also showed that solutions of Y74W apo-pseudoazurin ranging from 1 to 10 mg/mL in 4.3 M urea are monodisperse, with an average hydrodynamic radius of 3.6 nm, consistent with a partially unfolded monomer of ~13 kDa (the hydrodynamic radius of native protein in buffer A, in the absence of urea is ~2 nm). Finally, the equilibrium unfolding curve was identical when carried out in the presence of 50 mM EDTA, confirming that the transition does not reflect denaturation of a mixture of holo- and apo-protein.

Properties of Partially Unfolded Y74W Apo-Pseudoazurin. Complex equilibrium unfolding behavior has been observed for a number of proteins (*10*, *54*−*56*). These proteins usually contain multiple domains with different stabilities, and their unfolding behavior can be simply explained by sequential domain unfolding. Since Y74W apo-pseudoazurin contains only a single domain composed of two interwound Greek key motifs, it is difficult to imagine a plausible division of the structure into independent folding domains. Although the two α-helices could possibly form a domain independent of the *β*-sheets, the free-energy difference upon their unfolding is unlikely to be as substantial as that observed. Moreover, analysis of the X-ray structure of wild-type pseudoazurin indicates that the helices pack tightly against the *β*-barrel, making numerous interactions and thus a separate division of the molecule into distinct folding domains is unlikely (*49*).

To assess the conformational properties of partially folded Y74W apo-pseudoazurin in more detail a variety of approaches were employed, including far-UV CD, near-UV CD, steady-state fluorescence, time-resolved fluorescence, fluorescence anisotropy measurements, and 1D ^{1}H NMR. A significant residual signal is retained in the far-UV CD spectrum of Y74W apo-pseudoazurin in 4.3 M urea (Figure 5a), suggesting that at least some secondary structure persists

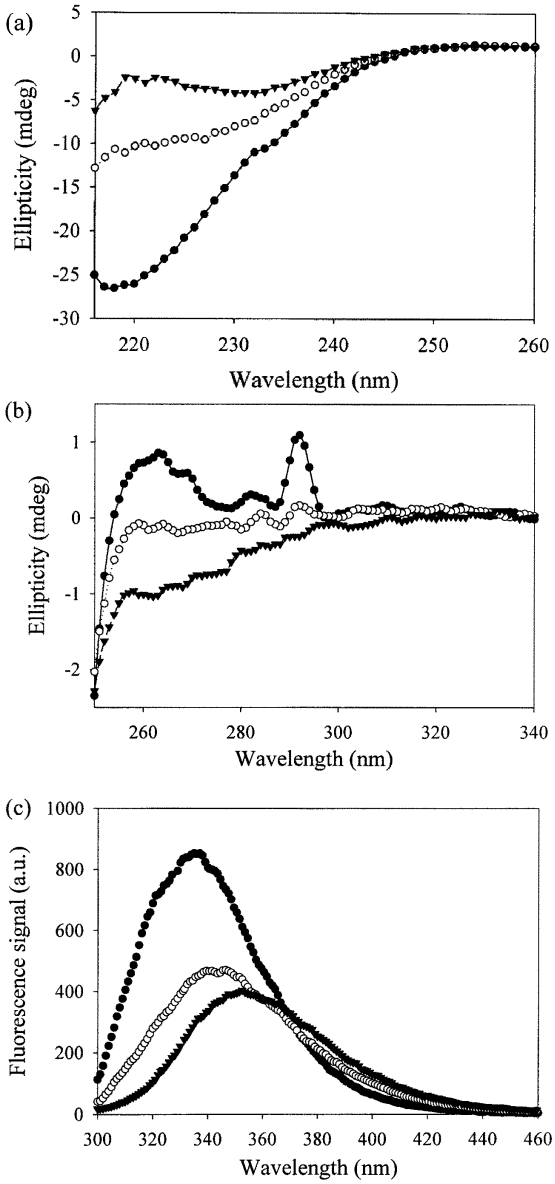

FIGURE 5: Conformational properties of partially unfolded Y74W apo-pseudoazurin. (a) Far-UV CD; (b) near-UV CD; (c) tryptophan fluorescence emission spectra. In each case, the signal of the native protein (●); partially folded species in 4.3 M urea (○); and protein denatured in 8 M urea (▼) are shown. Spectra were acquired in buffer A at 15 °C.

in this species. By contrast, the signal in the near-UV CD is almost completely abolished in 4.3 M urea (Figure 5b), indicating that species populated in 4.3 M urea lack the fixed tertiary interactions involving tryptophan and tyrosine residues that characterize the native state. A large decrease in tryptophan fluorescence intensity and increase in λ_{max} from 335 nm to 340 nm (Figure 5c), coupled with the lack of significant chemical shift dispersion observed in the 1D ^{1}H NMR spectrum of this species (Figure 6), are also consistent with partial unfolding of the protein in 4.3 M urea. Interestingly, however, resonances in the ^{1}H NMR spectrum of Y74W apo-pseudoazurin in 4.3 M urea are much sharper than typically observed for partially unfolded species in intermediate exchange (*57*, *58*) on the NMR time scale, suggesting that if more than one species is populated in Y74W apo-pseudoazurin in 4.3 M urea, they are in rapid exchange.

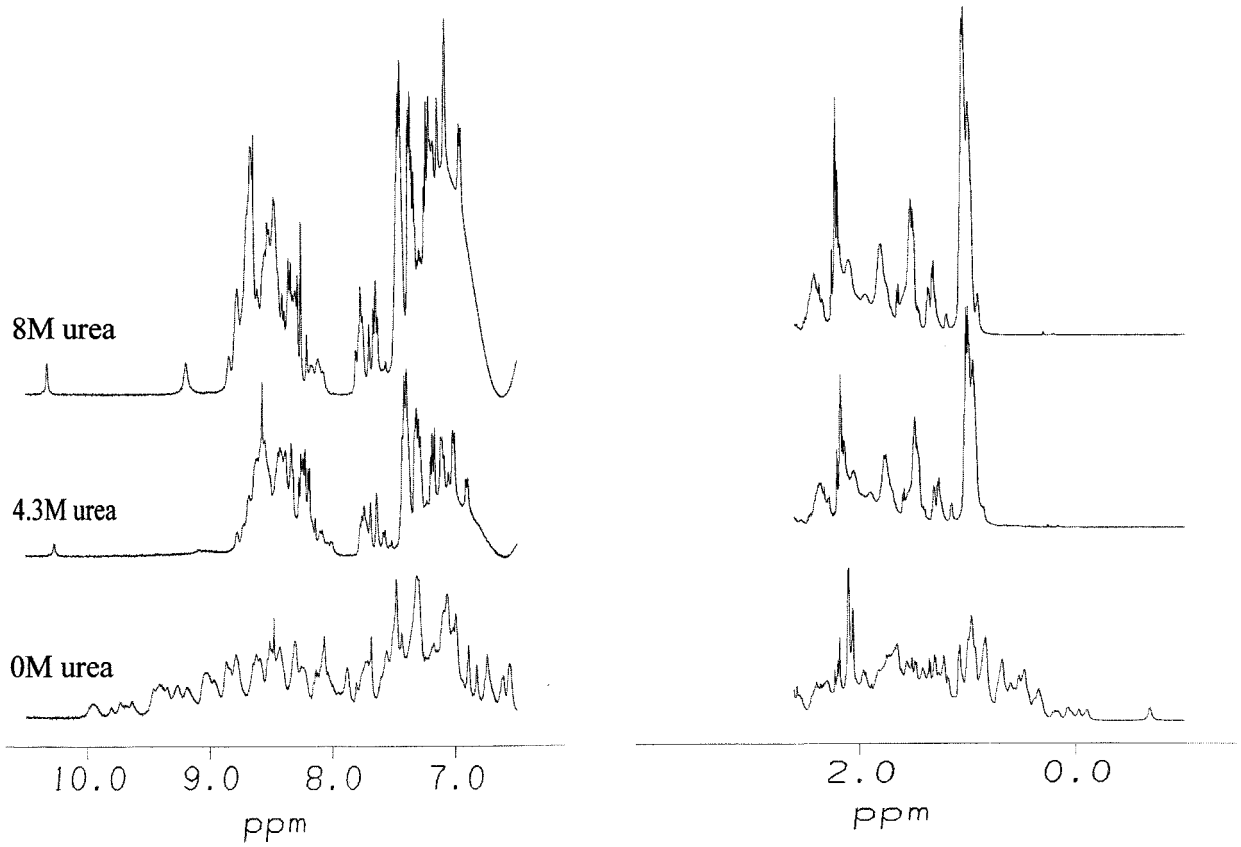

FIGURE 6: One-dimensional ^{1}H NMR spectra of Y74W apo-pseudoazurin in 0 M urea (lower spectrum), 4.3 M urea (middle spectrum), and 8 M urea (top spectrum) at pH 7.0, 15 °C and in 0.5 M Na_2SO_4.

Table 1: Time Resolved Fluorescence Decay Parameters of Y74W Apo-Pseudoazurin as a Function of Denaturant Concentration[a]

urea (M)	a_1 (%)	τ_1 (ns)	a_2 (%)	τ_2 (ns)	a_3 (%)	τ_3 (ns)	χ^2
0			13	1.521 ± 0.054	87	5.156 ± 0.272	1.04
1			9	1.285 ± 0.052	91	5.104 ± 0.022	1.14
2			12	1.825 ± 0.083	88	5.114 ± 0.031	1.11
3			17	1.648 ± 0.069	83	5.114 ± 0.042	1.04
3.5	1	0.026 ± 0.009	10	1.360 ± 0.075	89	4.985 ± 0.035	1.00
4	2	0.034 ± 0.002	10	1.273 ± 0.069	88	4.944 ± 0.033	1.11
4.5	3	0.039 ± 0.017	10	1.146 ± 0.071	87	4.859 ± 0.036	1.01
5	5	0.037 ± 0.001	15	1.223 ± 0.057	80	4.614 ± 0.040	1.24
5.5	5	0.039 ± 0.001	16	1.199 ± 0.049	79	4.536 ± 0.033	1.09
6	1	0.051 ± 0.008	14	1.095 ± 0.046	85	4.498 ± 0.035	1.10
7	1	0.039 ± 0.031	17	1.199 ± 0.129	82	4.536 ± 0.068	1.10
8	2	0.038 ± 0.003	17	1.201 ± 0.045	81	4.577 ± 0.037	1.02

[a] a_x (%) is the contribution to the total fluorescence lifetime of the component with characteristic lifetime τ_x (nanoseconds).

Fluorescence Lifetime and Time-Resolved Anisotropy Measurements. To gain further insight into the conformational properties of Y74W apo-pseudoazurin, fluorescence lifetime and anisotropy measurements were carried out. The time-resolved fluorescence lifetime data shown in Table 1 indicate that Y74W apo-pseudoazurin exhibits an essentially biexponential fluorescence decay over the entire range of urea concentrations studied, with only a very small contribution (<5%) of a third rapid decay constant (~30 ps) above 3.5 M urea. In the native-state (0−2.5 M urea) fluorescence decays with characteristic lifetimes of approximately 5.1 and 1.5 ns with amplitudes of ~85 and ~15%, respectively, are observed. Multiple lifetimes in single tryptophan-containing proteins have been observed in other proteins and have been attributed to multiple conformations of the tryptophan side chain (*59*, *60*), multiple microstates or alternative protein conformations (*61*, *62*). There have been a few reports of single-exponential tryptophan fluorescence decays in native proteins (*50*, *63*, *64*), but these are exceptional. Between 3.5 and 4.5 M urea, the fluorescence decay lifetimes decrease to values of about 4.9 and 1.2 ns, consistent with increased solvent exposure of the fluorophore and the decrease in steady state fluorescence emission intensity. In the unfolded state (>6 M urea), these two decay constants decrease further to values of about 4.5 and 1.1 ns consistent with increased solvent accessibility of the tryptophan as the intermediate(s) unfold(s). The relative amplitudes of these two components remain approximately constant versus denaturant concentration (~85 and ~15%, respectively).

To analyze the equilibrium intermediate species further, specifically in terms of its heterogeneity, compactness and motional freedom of the tryptophan residue, time-resolved fluorescence anisotropy measurements were also analyzed over a wide range of urea concentrations (Figure 7). The anisotropy experiments were performed on two time scales (summarized in Tables 2 and 3) in order to accurately determine both the slower decay rates which reflect the global rotation of the whole protein (25 ns time scale) and faster decay rates (5 ns time scale) which reflect localized tryptophan freedom or segmental motion. Under native conditions, the decay of fluorescence anisotropy is described by a single exponential (Figure 7a), confirming the presence of a unique native conformation under these experimental conditions. The time constant of the fluorescence anisotropy decay of the native protein increases with increasing urea

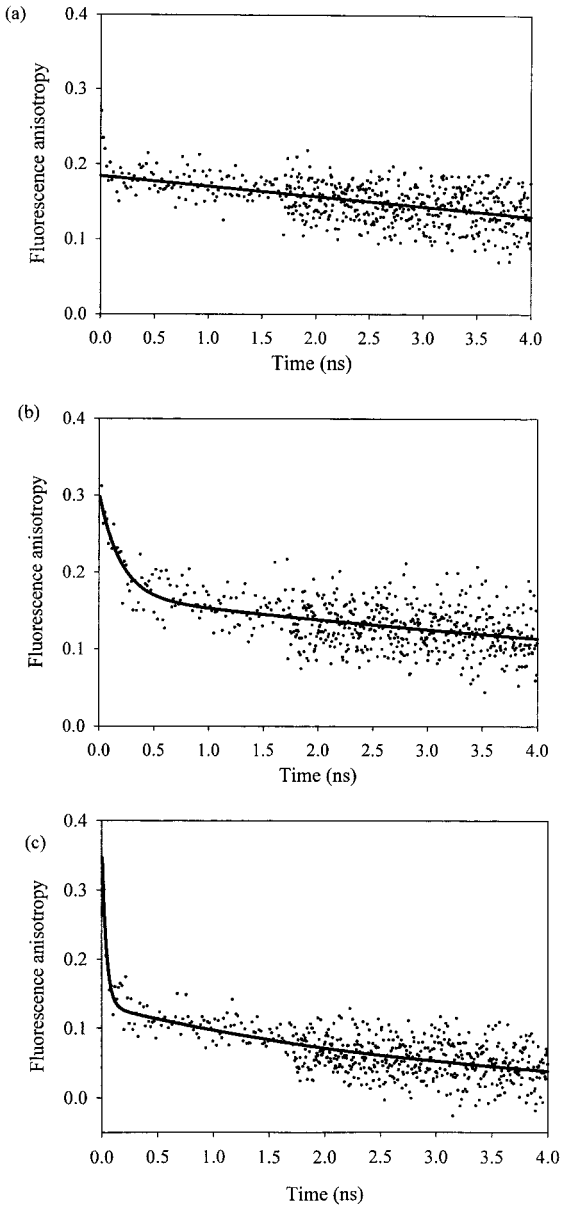

FIGURE 7: Fluorescence anisotropy decays of Y74W apo-pseudoazurin in the presence of (a) 0 M urea, (b) 4.5 M urea, and (c) 8 M urea in buffer A at 15 °C. The solid line shows fits of the data to a single exponential (a) and biexponential (b and c) functions.

concentration from a value of 6.4 ns in 0 M urea to 10.2 ns in 2.0 M urea (Table 2). The former measurement agrees well with the rotational correlation time previously calculated from ^{15}N relaxation time measurements of native wild-type pseudoazurin (6.3 ns) (G. S. Thompson, Y.-C. Leung, C. Redfield, S. J. Ferguson, and S.E.R., *Protein Sci.*, in press). This value is also in good agreement with rotational correlation times observed for other small proteins (*46*, *65*). For a globular protein the rotational correlation time (ϕ) is given by

$$\phi = \frac{\eta M}{RT}(\bar{\nu} + h) \qquad (7)$$

where η is the viscosity of the solvent (buffer A without urea measured to be 1.29×10^{-3} Pa s at 15 °C), M is the molecular weight of the protein, $\bar{\nu}$ is the specific volume of the protein, and h is the degree of hydration (taken to be 0.3 cm^3/g protein) (*66*). For a spherical protein of molecular mass 13 366 Da and specific volume of 0.7 cm^3/g of apo-pseudoazurin, the rotational correlation time is calculated to be 7.8 ns, in good agreement with the measured value in 0 M urea. Although the longer correlation time which corresponds to global protein motion cannot be accurately determined from the short time-scale data in Table 3, these data confirm that there is no fast anisotropy decay component in the range 0−2.0 M urea, indicating that the tryptophan residue is in a fixed position (possibly hydrogen bonded) in the native protein. The emergence of a significant contribution (50%) from a fast decay component (0.035 ns) in 3.5 M urea is indicative of rapid rotation of the tryptophan residue, suggesting that the indole ring is no longer fixed in the intermediate species. Importantly, the observation of only a single decay component corresponding to global protein motion suggests that if more than one species is populated in 4.3 M urea, then theses species must have very similar correlation times. In addition, the increase in the long correlation time from 13.2 to 18.1 ns between 3.5 and 4.5 M urea suggests that partially unfolded Y74W apo-pseudoazurin is expanded compared to the native state, but remains globally compact.

As the urea concentration is increased further from 5 to 8 M, data from both the long and short time-scale experiments show that the correlation time for the global motion of the protein increases until it can no longer be measured accurately ($>\sim$20 ns). The contribution of the fast ($<$100 ps) anisotropy decay increases to approximately 70% in this urea concentration range and reflects the increased rotational freedom of the tryptophan residue in the denatured state. The data in Tables 2 and 3 also show a $\sim$30% contribution to the anisotropy decay time constant of approximately 3 ns, which may arise from segmental motion in the vicinity of the tryptophan residue in the unfolded protein. Importantly, anisotropy decays between 3.5 and 4.5 M urea could not be fitted satisfactorily to a linear combination of the anisotropy decays of the native and denatured states, confirming that the unique fluorescence characteristics at intermediate concentrations of urea reflect the presence of novel, but structurally similar partially folded species populated during unfolding.

In native Y74W apo-pseudoazurin, the tryptophan is fixed in the protein resulting in a single-exponential decay of fluorescence anisotropy on a time scale commensurate with global protein rotation and a calculated cone angle of 0° (Table 3). However, under conditions where one or more intermediates are populated, there is a 50% contribution of the rapid decay component (Table 3) which results in a calculated cone angle of about 38° that remains constant between 3.5 and 4.5 M urea. This is consistent with only partial unfolding in the vicinity of the tryptophan residue over this range of urea concentrations.

Structural Properties of Y74W Apo-Pseudoazurin Peptides. To test the hypothesis that the tryptophan corner may persist in partially folded apo-pseudoazurin, three peptides of increasing lengths that contained Trp74 were synthesized and their ability to fold in isolation analyzed. The peptides were 11 (pep1), 19 (pep2), and 30 (pep3) residues in length, and encompassed residues 69−75 (the tyrosine corner only), 63−77 (the tyrosine corner plus β-strands VI and VII), or 52−77 (the tyrosine corner plus β-strands V, VI, and VII),

Table 2: Time Resolved Fluorescence Anisotropy Decay Parameters of Y74W Apo-Pseudoazurin as a Function of Denaturant Concentration Acquired on a 25 ns Time Scale[a]

urea (M)	initial anisotropy, r_o	a_1 (%)	τ_1 (ns)	a_2 (%)	τ_2 (ns)	a_3 (%)	τ_3 (ns)
0	0.15					100	6.37 ± 0.47
1	0.20					100	7.49 ± 1.52
2	0.19					100	10.19 ± 2.15
3	0.19					100	11.87 ± 0.47
3.5	0.16					100	13.22 ± 0.86
4	0.17			24	0.516 ± 0.182	76	17.83 ± 1.76
4.5	0.17			36	0.327 ± 0.094	66	18.08 ± 1.51
5	0.27	63	0.045 ± 0.009	19	1.06 ± 0.30	18	10.76 ± 3.18
5.5	0.26	54	0.052 ± 0.021	35	1.05 ± 0.40	11	8.72 ± 3.23
6	0.20	35	0.058 ± 0.056	35	0.506 ± 0.298	30	5.90 ± 1.01
7	0.18	44	0.109 ± 0.100	56	1.00 ± 0.89		
8	0.17	41	0.136 ± 0.053	59	1.62 ± 0.37		

[a] a_x (%) is the contribution to the total anisotropy decay of the component with characteristic decay time τ_x (nanoseconds).

Table 3: Time Resolved Fluorescence Anisotropy Decay Parameters of Y74W Apo-Pseudoazurin as a Function of Denaturant Concentration Acquired on a 5 ns Time Scale[a]

urea (M)	initial anisotropy r_o	a_1 (%)	τ_1 (ns)	a_2 (%)	τ_2 (ns)	θ (deg)
0	0.17			100	10.32 ± 0.52	0
1	0.16			100	20.44 ± 1.34	0
2	0.17			100	10.00 ± 1.10	0
3	0.17			100	9.00 ± 0.87	0
3.5	0.32	47	0.035 ± 0.006	53	11.08 ± 0.98	36
4	0.29	52	0.054 ± 0.007	48	10.89 ± 0.96	39
4.5	0.31	48	0.096 ± 0.010	52	12.17 ± 1.24	37
5	0.31	68	0.083 ± 0.006	32	3.63 ± 0.20	-
5.5	0.33	73	0.089 ± 0.006	27	3.18 ± 0.24	-
6	0.30	67	0.040 ± 0.005	33	3.47 ± 0.24	-
7	0.29	69	0.096 ± 0.007	31	2.30 ± 0.12	-
8	0.34	68	0.069± 0.009	32	3.35 ± 0.17	-

[a] a_x (%) is the contribution to the total anisotropy decay of the component with characteristic decay time τ_x (nanoseconds).

respectively (see Figure 1a). As judged by far-UV CD, tryptophan fluorescence, 1D ^{1}H NMR, and fluorescence lifetime and anisotropy measurements, none of the peptides contained significant nonrandom structure in buffer A at 15 °C, suggesting that nonlocal interactions are important for stabilization of the intermediate species in the intact protein.

DISCUSSION

The introduction of a tryptophan residue into the tyrosine corner of pseudoazurin from *Paracoccus pantotrophus* has allowed us to probe the folding properties of the apo-protein. ^{1}H NMR, CD, and fluorescence anisotropy data point to the mutant possessing a highly nativelike structure (both in the presence and absence of stabilizing Na_2SO_4). The mutant protein is compact (having a rotational correlation time similar to that of the wild-type protein), has nativelike secondary structure (as judged by far-UV CD) and fixed tertiary contacts (revealed by near-UV CD). Moreover, the side chain of the newly introduced tryptophan residue is likely to be buried within the hydrophobic core of the native protein (the mutant has a substantial near-UV CD signal around 290 nm, a relatively long fluorescence lifetime and a blue-shift in λ_{max}). Accordingly, Tyr74 has less than 2% of its surface area exposed to solvent in wild-type apo-pseudoazurin [calculated using DSSP (*67*)]. Furthermore, the lack of a rapid fluorescence anisotropy decay lifetime in the absence of urea indicates that the tryptophan residue cannot freely rotate in the native protein suggesting that the newly introduced tryptophan residue might be hydrogen bonded. This is supported by a preliminary ultraviolet resonance Raman (UVRR) study which indicates an ω17 peak at 868 cm^{-1} (*68*). The ratio of the two peaks in the ω7 fermi doublet at 1360/1340 cm^{-1} is ∼1.0 also confirms that Trp74 is in a hydrophobic environment as would be expected under native conditions (*69*) (J. Clarkeson, S.J., S.E.R., and D.A.S., unpublished data), raising the possibility that replacement of the tyrosine for tryptophan has not disrupted the tyrosine corner. Interestingly, tryptophan corners are found in other Greek key proteins (*39*).

Although Y74W apo-pseudoazurin adopts a nativelike fold, its unfolding transition displays a distinct deviation from the two-state behavior previously observed for the wild-type protein at equilibrium both in the presence (*27*) and absence of stabilizing Na_2SO_4 (Supporting Information, Figure 2). One or more partially unfolded species are populated in Y74W apo-pseudoazurin between 3.5 and 4.5 M urea in the presence of 0.5 M Na_2SO_4. Whether such species are populated in the absence of stabilizing Na_2SO_4 could not be definitively assessed, however, since the native apo-protein is too unstable to permit accurate measurements in the absence of Na_2SO_4 (see Supporting Information, Figure 2b). In the presence of 0.5 M Na_2SO_4, partially folded Y74W apo-pseudoazurin retains significant residual nonrandom structure involving the newly introduced tryptophan residue. Interestingly, however, substitution of tryptophan for Phe56 (which lies in strand V) in apo-pseudoazurin results in a protein that denatures with an apparently two-state transition with a $\Delta G_{un}^{H_2O}$ value of 27.8 (±1.3) kJ/mol and an m_{un} value of 8.29 (±0.39) kJ/mol M in good agreement with the data for the wild-type protein (S. J., and S. E. R., unpublished data). This suggests that the effect of introducing a trytophan residue into apo-pseudoazurin is context dependent, and that substitution of tryptophan in the tyrosine corner perturbs the stability of intermediate(s) with respect to native and unfolded species so that it becomes visibly populated at intermediate concentrations of urea. Previous kinetic studies of unfolding of the wild-type protein using double mixing far-UV CD experiments have also shown the presence of an unusually stable folding intermediate that is maximally populated (relative to the native and denatured states) between 4.5 and 4.9 M urea under identical conditions to those used here (*27*). Whether these species are related, however, will require further analysis, for example, using

hydrogen exchange labeling or site-directed mutagenesis experiments (*5*, *6*, *13*).

Detailed analysis of the conformation of Y74W apo-pseudoazurin in 4.3 M urea revealed a partially folded ensemble which retains significant residual secondary structure but lacks the fixed tertiary interactions characteristic of the native state. Nevertheless, this species does not appear to be typical of the partially folded molten globules observed in other proteins (*5*, *6*, *13*), in that its ^{1}H NMR spectrum has sharp resonances [rather than the line broadening usually found for other molten globule states (*57*, *58*)] and this species does not bind ANS, indicating the absence of exposed hydrophobic surface area. Interestingly, partially folded intermediates of other proteins including bovine pancreas trypsin inhibitor (under some conditions) (*70*, *71*) and apo-myoglobin (*72*) also fail to bind ANS. In summary, our model for the unfolding intermediate(s) of Y74W apo-pseudoazurin points to population of one or more species that, on average, are compact (with a rotational correlation time of 13.2−18.1 ns) and contain residual secondary structure and significant nonrandom structure involving the newly introduced tryptophan residue. Although the number of species populated in 4.3 M urea cannot be deduced from the data presented above, the ensemble of species populated presumably possesses similar overall properties as reflected in the single anisotropy fluorescence decay observed. The data are consistent with retention of the proposed β-zipper involving β-strands VI and VII that juxtapose the tryptophan corner, possibly stabilized by long-range interactions within the compact globule. Consistent with this, synthetic peptides encompassing this region are not structured in isolation under the chosen conditions. This model for partially folded Y74W apo-pseudoazurin is supported by the small red-shift in the λ_{max} of tryptophan fluorescence emission, indicating that the tryptophan is not completely solvent exposed, a fluorescence lifetime between those of the native and denatured states, and restricted tryptophan motion reflected by a semicone angle of ∼38° that remains constant between 3.5 and 4.5 M urea.

The data presented here not only pinpoint residual structure in partially folded Y74W apo-pseudoazurin but also suggest that the unfolded state of the protein in 8 M urea also retains significant nonrandom structure involving the tryptophan residue. Thus, the steady-state fluorescence signal in 8 M urea shows significant intensity around ∼335 nm, possibly indicating retention of residual structure involving a buried tryptophan residue, in addition to the red-shifted peak indicative of solvent exposure of the tryptophan in the denatured state (Figure 5c). Segmental motion involving the tryptophan residue is also retained, even in high denaturant concentrations, as determined by fluorescence anisotropy (Table 2). Consistent with this, a contribution from aromatic residues in the far-UV CD spectrum between 230 and 240 nm is observed in 8 M urea (Figure 5a).

The observation that Y74W apo-pseudoazurin is not fully unfolded even in the presence of 8 M urea is intriguing. Reports are emerging from other workers about residual structure in the unfolded states of other proteins, including lysozyme (*73*); the amino-terminal domain of the phage 434 repressor (*74*); apo-myoglobin (*75*); staphylococcal nuclease II (*76*); and the *Drosophila* (drkN) SH3 domain (*77*). The presence of nonrandom structure in unfolded proteins has an important impact on the conformational search required to produce the fully folded native state. The retention of residual nativelike structural elements may shape the energy landscape, as structured species in the unfolded ensemble will entropically favor folding. Removal of solvent upon dilution of denaturant could enhance the stability of these regions, around which the remaining structural elements could then form. In some proteins, however, there is little or no relationship between residual interactions in denatured proteins or partially folded species and the folding transition to the native state (*78*−*80*). The relevance of residual interactions in the denatured state therefore might be protein specific. In the case of Y74W apo-pseudoazurin, it is intriguing that the residual structure observed in the partially folded and unfolded states in 8 M urea might involve the tryptophan corner that has been postulated to be important in early events in folding of Greek key proteins and shown to be important in folding of fibronectin type III domains (*40*). Interestingly, replacement of Tyr74 in pseudoazurin with alanine, serine, or phenylalanine resulted in either lethal proteins or proteins that could not be expressed (data not shown), suggesting that the interactions in the tyrosine corner are essential for the generation and/or for maintenance of the integrity of this cupredoxin fold. Further kinetic experiments are now planned to test this hypothesis.

ACKNOWLEDGMENT

We gratefully acknowledge Keith Ainley for preparing Y74W apo-pseudoazurin, Maureen Pitkeathly (Oxford Centre for Molecular Sciences) for peptide synthesis, Fadi Aboushakra (Micromass UK Ltd) for ICP-MS measurements, Neil Kad for help with dynamic light scattering, Andy Baron for performing ultracentrifugation experiments, Pete Mawer for performing viscosity measurements, Steve Homans and Gary Thompson for help with NMR, and Alan Berry for construction of Figure 1. We thank the Radford group for critically reading the manuscript. We also thank Chris Dobson for providing access to equipment in the early stages of J.S.R.'s studentship and for helpful discussions.

SUPPORTING INFORMATION AVAILABLE

Two figures of equilibrium unfolding of Y74W apo-pseudoazurin measured by tryptophan fluorescence and far-UV CD and effect of 0.5 M Na_2SO_4 on the equilibrium unfolding transactions of wild-type and Y74W apo-pseudoazurin. This material is available free of charge via the Internet at http://pubs.acs.org.

REFERENCES

1. Jackson, S. (1998) *Folding Des. 3*, R81−R91.
2. Khorasanizeadeh, S., Peters, I. D., Butt, T. R., and Roder, H. (1996) *Nat. Struct. Biol. 3*, 193−205.
3. Park, S. H., O'Neil, K. T., and Roder, H. (1997) *Biochemistry 47*, 14277−14283.
4. Ferguson, N., Capaldi, A. P., James, R., Kleanthous, C., and Radford, S. E. (1999) *J. Mol. Biol. 286*, 1597−1608.
5. Colón, W., and Roder, H. (1996) *Nat. Struct. Biol. 3*, 1019−1025.
6. Jennings, P. A., and Wright, P. E. (1993) *Science 262*, 892−896.
7. Peng, Z.-Y., and Kim, P. S. (1994) *Biochemistry 33*, 2136−2141.
8. Wu, L. C., Peng, Z.-Y., and Kim, P. S. (1995) *Nat. Struct. Biol. 2*, 281−286.
9. Chamberlain, A. K., Handel, T. M., and Marquesee, S. (1996) *Nat. Struct. Biol. 3*, 782−787.

10. Mayr, E.-M., Jaenicke, R., and Glockshuber, R. (1997) *J. Mol. Biol. 269*, 260−269.
11. Webb, T., Jackson, P. J., and Morris, G. E. (1997) *Biochem. J., 321*, 83−88.
12. Ayed, A., and Duckworth, H. W. (1999) *Protein Sci, 8*, 1116−1126.
13. Chamberlain, A. K., and Marquesee, S. (1997) *Structure 5*, 859−863.
14. Hamada, D., Segwada, S.-I., and Goto, Y. (1996) *Nat. Struct. Biol. 3*, 868−873.
15. Carlsson, U., and Jonsson, B.-H. (1995) *Curr. Opin. Struct. Biol. 5*, 482−487.
16. Capaldi, A. P., and Radford, S. E. (1998) *Curr. Opin. Struct. Biol. 8*, 86−92.
17. Schindler, T., Herrler, M., Marahiel, M. A., and Schmid, F. X. (1995) *Nat. Struct. Biol. 2*, 663−673.
18. Schönbrunner, N., Pappenberger, G., Scharf, M., Engels, J., and Keifhaber, T. (1997) *Biochemistry 36*, 9057−9065.
19. Vigeura, A. R., Martinez, J. C., Filimonov, W., Mateo, P. L., and Serrano, L. (1993) *Biochemistry 33*, 2141−2150.
20. Riddle, D. S., Santigo, J. V., Bray Hal, S. T., Doshi, N., Grantcharova, V., Yi, Q., and Baker D. (1997) *Nat. Struct. Biol. 4*, 805−809.
21. Plaxco, K. W., Morton, C. J., Guijarro, J. I., Pitkeathly, M., Campbell, I., and Dobson, C. M. (1998) *Biochemistry 37*, 2529−2537.
22. Plaxco, K. W., Spitzfaden, C., Campbell, I., and Dobson, C. M. (1996) *Proc. Natl. Acad. Sci. U.S.A. 93*, 10703−10706.
23. Plaxco, K. W., Spitzfaden, C., Campbell, I., and Dobson, C. M. (1997) *J. Mol. Biol. 270*, 763−770.
24. Clarke, J., Hamill, S. J., and Johnson, C. M. (1997) *J. Mol. Biol. 270*, 771−778.
25. Parker, M. J., and Clarke, A. R. (1997) *Biochemistry 36*, 5786−5794.
26. Heidary, D. K., Gross, L. A., Roy, M., and Jennings, P. A. (1997) *Nat. Struct. Biol. 4*, 725−731.
27. Capaldi, A. P., Ferguson, S. J., and Radford, S. E. (1999) *J. Mol. Biol. 286*, 1621−1632.
28. Clark, P. L., Liu, Z.-P., Rizo, J., and Gierasch, L. M. (1997) *Nat. Struct. Biol. 4*, 883−886.
29. Clark, P. L., Weston, B. F., and Gierasch, L. M. (1998) *Folding Des. 3*, 401−412.
30. Ropson, I. J., Gordon, J. I., and Frieden, C. (1990) *Biochemistry 29*, 9591−9599.
31. Ropson, I. J., Gordon, J. I., Cistola, D. P., and Frieden, C. (1992) in *Techniques in Protein Chemistry III* (Angeletti, R. A., Ed.) pp 437−443, Academic Press, New York.
32. Ropson, I. J., and Dalessio, P. M. (1997) *Biochemistry 36*, 8594−8601.
33. Clarke, J., Cota, E., Fowler, S. B., and Hamill, S. J. (1999) *Structure 7*, 1145−1153.
34. Richardson, J. (1977) *Nature 268*, 495−500.
35. Hazes, B., and Hol, W. G. J. (1992) *Proteins: Struct., Funct., Genet. 12*, 278−298.
36. Muñoz, V., Thompson, P. A., Hofrichter, J., and Eaton, W. A. (1997) *Nature 390*, 196−1997.
37. Blanco, F. J., Ramirez-Alvarado, M., and Serrano, L. (1998) *Curr. Opin. Struct. Biol. 8*, 107−111.
38. Yi, Q., Bystroff, C., Rajagopal, P., Klevit, R. E., and Baker, D. (1998) *J. Mol. Biol. 283*, 293−300.
39. Hemmingson, J. M., Gernert, K. M., Richardson, J. S., and Richardson, D. C. (1994) *Protein Sci. 3*, 1927−1937.
40. Hamill, S. J., Cota, E., Chothia, C., and Clarke, J. (2000) *J. Mol. Biol. 295*, 641−649.
41. Kunkel, T. A., Roberts, J. D., and Zakour, R. A. (1987) *Methods Enzymol. 154*, 367−370.
42. Leung, Y. C., Chan, C., Reader, J. S., Willis, A. C., van Spanning, R., Ferguson, S. J., and Radford, S. E. (1997) *Biochem. J. 321*, 699−705.
43. Santoro, M., and Bolen, D. W. (1988) *Biochemistry 27*, 8063−8068.
44. Kinosita, K., Kawato, S., and Ikegami, A. (1977) *Biophys. J. 20*, 289−305.
45. Lipari, G., and Szabo, A. (1980) *Biophys. J. 30*, 489−506
46. Steiner, R. F., (1991) in *Topics in Fluorescence Specotroscopy, Volume 2: Principles* (Lakowicz, J. R., Eds.) Plenum, New York.
47. Ramirez-Almarado, M., Blanco, F. J., and Serrano, L. (1996) *Nat. Struct. Biol. 3*, 604−612.
48. Reader, J. S. (1998) D. Phil., University of Oxford.
49. Williams, P. A., Fülop, V., Leung, Y.-C., Chan, C., Moir, J. W. B., Howlett, G., Ferguson, S. J., Radford, S. E., and Hajdu, J. (1995) *Nat. Struct. Biol. 2*, 975−982.
50. Hutnik, C. M., and Szarbo, A. G. (1989) *Biochemistry 28*, 3923−3939.
51. Sanz J. M., and Fersht, A. R. (1993) *Biochemistry 32*, 13584−13592.
52. Myers, J. K., Pace, C. N., and Scholtz, J. M. (1995) *Protein Sci. 4*, 2138−2148.
53. Filiminov, V. V., Prieto, J., Martinez, J. C., Bruix, M., Mateo, P. L., and Serrano, L. (1993) *Biochemistry 32*, 12906−12921.
54. Hornemann, S., and Glockshuber, R. (1996) *J. Mol. Biol. 261*, 614−618.
55. Wenk, M., Baumgartner, R., Holak, T. A., Huber, R., Jaenicke, R., and Mayr, E.-M. (1999) *J. Mol. Biol. 286*, 1533−1545.
56. Wieligmann, K., Mayr, E.-M., and Jaenicke, R. (1999) *J. Mol. Biol. 286*, 989−994.
57. Baum, J., Dobson, C. M., Evans, P. A., and Hanley, C. (1989) *Biochemisty 28*, 7−13.
58. Alexandrescu, A. T., Evans, P. A., Pitkeathly, M., Baum, J., and Dobson, C. M. (1993) *Biochemistry 32*, 1707−1718.
59. Chen, L. X.-Q., Longworth, J. W., and Fleming, G. R. (1987) *Biophys J. 51*, 865−873.
60. Chen, R. F., Knutson, J. R., Ziffer, H., and Porter, D. (1991) *Biochemistry 30*, 5184−5195.
61. Chabbert, M., Hillen, W., Hansen, D., Takahashi, M., and Bouesquet, J.-A. (1992) *Biochemistry 31*, 1951−1960.
62. Kim, S.-J., Chowdhury, F. N., Younatahn, W. S. E. S., Rosso, P. S., and Barkley, M. D. (1993) *Biophys. J. 65*, 215−226.
63. Gilardi, G., Mei, G., Rosato, N., Canters, G. W., Finazziargro, A. (1994) *Biochemistry 33*, 1425−1432.
64. Swimanthan, R., Nath, U., Udgaonkar, J. B., Periasamy, N., and Krishnamoorthy, G. (1996) *Biochemistry 35*, 9150−9157.
65. Eftink, M. R., Gryczynski, I., Wiczk, W., Laczko, G., and Lakowicz, J. R. (1991) *Biochemistry 30*, 8945−8953.
66. Lakowicz, J. R. (1983) *Principles of Fluorescence Spectroscopy*, Plenum, New York.
67. Kabsch, W., and Sander, C. (1983) *Biopolymers 22*, 2577−2637.
68. Miura, T., Takeuchi, H., and Harada, I. (1988) *Biochemistry* 27, 88−94.
69. Harada, I., Miura, T., and Takeuchi, H. (1986) *Spectrochim. Acta 42A*, 307−312.
70. Darby, N., and Creighton, T. (1993) *J. Mol. Biol. 232*, 873−896.
71. Ferrer, M., Barany, G., and Woodward, C. (1995) *Nat. Struct. Biol. 2*, 211−217.
72. Colonna, G., Balestrieri, C., Bismuto, E., Servillo, L., and Irace, G. (1982) *Biochemistry 21*, 212−215.
73. Evans, P. A., Topping, K. D., Woolfson, D. N., and Dobson, C. M. (1991) *Proteins: Struct., Funct., Genet. 9*, 248−266.
74. Neri, D., Wider, G., and Wuthrich, K. (1992) *Proc. Natl. Acad. Sci. U.S.A. 89*, 4397−4401.
75. Griko, Y., and Privalov, P. L. (1994) *J. Mol. Biol. 235*, 1318−1325.
76. Gillespie, J. R., and Shortle, D.(1997) *J. Mol. Biol. 268*, 170−184.
77. Mok, Y.-K., Kay, C. M., Kay, L. E., and Forman-Kay, J. (1999) *J. Mol. Biol. 289*, 619−638.
78. Fuijiwara, K., Arai, M., Shimizu, A., Ikeguchi, M., Kuwajima, K., and Sugai, S. (1999) *Biochemistry 38*, 4455−4463.
79. Blanco, F. J., Serrano, L., and Forman-Kay, J. D. (1998) *J. Mol. Biol. 284*, 1153−1164.
80. Villegas, V., Martínez, J. C., Avilés, F. X., and Serrano, L. (1998) *J. Mol. Biol. 283*, 1027−1036.
81. Kraulis, P. J. (1991) *J. Appl. Crystallogr. 24*, 946−950.

BI9923959